Journal of Materials Chemistry C

ROYAL SOCIETY OF CHEMISTRY

PAPER

View Article Online
View Journal | View Issue

Cite this: J. Mater. Chem. C, 2024, 12, 8508

Mechanically-sensitive fluorochromism by molecular domino transformation in a Schiff base crystal†

Toshiyuki Sasaki, *[a] Takanori Nakane, [b] Akihiro Kawamoto, [b] Yakai Zhao, [cd] Yushi Fujimoto, [e] Tomohiro Nishizawa, [f] Nabadeep Kalita, [g] Seiji Tsuzuki, *[h] Fuyuki Ito, *[e] Upadrasta Ramamurty, *[cd] Ranjit Thakuria *[g] and Genji Kurisu *[bij]

Received 29th January 2024,
Accepted 11th April 2024

DOI: 10.1039/d4tc00406j

rsc.li/materials-c

The ability to make large changes in properties against small external stimuli is one of the key factors in sensing materials. Molecular domino transformation, *i.e.*, polymorphic transformation starting at a stimulated point and extending to the whole crystal, is an attractive phenomenon from this viewpoint. We recently found such a transformation for the first time in an organic crystal of 4-nitro-*N*-salicylideneaniline as one of the Schiff bases. In this study, quantitative evaluations were conducted on the mechanical stimulus and emission properties in the transformation of the crystal. Our results demonstrate the potential applicability of the crystal to the detection of even less than a few μN mechanical stimuli as an emission color change. A molecular level transformation mechanism revealed by microcrystal electron diffraction also contributes to the future development of the transformation-based materials.

Introduction

Molecular crystals can alter their properties in response to external stimuli by conversion of molecular structures, molecular arrangements, and/or crystal's components.[1–3] Various kinds of external stimuli, such as thermal,[4–9] mechanical,[10–15] light,[16–18] and vapor-based stimuli,[19–21] have been used to induce the conversion. Remarkable property changes and high sensitivity to external stimuli are reported; the tailoring of such changes can lead to fascinating sensing and actuation applications.

Molecular domino transformation (MDT), discovered and named by Ito *et al.* in a gold(I) complex in 2013,[11] is one such possible mechanism to achieve the desired characteristics. Not only is the transformation inducible by a small mechanical stimulus, but it also progresses from the initial point through the entire crystal autocatalytically. Such domino-like amplification of the response to mechanical stimulus enables the molecular crystals to detect mechanical stimuli with high sensitivity. However, MDT is reported only in a small number of molecular crystals hitherto.[9,11,12] Therefore, research on it has depended mostly on serendipity. For further rational development of sensing materials that use MDT as the main mechanism, fundamental understanding of it and in a wider variety of molecular systems is necessary.

Salicylideneaniline derivatives have been selected as a model system for this purpose in this study because of their remarkable polymorph-dependent fluorescence properties[22,23] as well as their easy availability *via* a condensation reaction of anilines and salicylaldehydes. Herein, we characterize MDT in a crystal of 4-nitro-*N*-salicylideneaniline (**1**). In addition to the evaluation of the emission characteristics by fluorescent microscopy, the mechanical sensitivity and the molecular level

[a] Japan Synchrotron Radiation Research Institute (JASRI), 1-1-1 Kouto, Sayo-cho, Sayo-gun, Hyogo 679-5198, Japan. E-mail: toshiyuki.sasaki@spring8.or.jp
[b] Institute for Protein Research, Osaka University, 3-2 Yamadaoka, Suita, Osaka 565-0871, Japan
[c] School of Mechanical and Aerospace Engineering, Nanyang Technological University, Singapore 639798, Singapore
[d] Institute of Materials Research and Engineering, Agency for Science, Technology and Research (A*STAR), Singapore 138634, Singapore
[e] Department of Chemistry, Institute of Education, Shinshu University, 6-ro, Nishinagano, Nagano, 380-8544, Japan
[f] Department of Biological Sciences, Yokohama City University, 1-7-29 Suehiro-cho, Tsurumi-ku, Yokohama 230-0045, Japan
[g] Department of Chemistry, Gauhati University, Guwahati 781014, Assam, India
[h] Department of Applied Physics, The University of Tokyo, Hongo 7-3-1, Bunkyo-ku, Tokyo, 113-8656, Japan
[i] JEOL YOKOGUSHI Research Alliance Laboratories, Graduate School of Frontier Biosciences, Osaka University, 1–3 Yamadaoka, Suita, Osaka 565-0871, Japan
[j] Institute for Open and Transdisciplinary Research Initiatives, Osaka University, 2-1 Yamadaoka, Suita, Osaka 565-0871, Japan

† Electronic supplementary information (ESI) available: Cryo-EM images, distribution of unit cell parameters, crystallographic data, powder X-ray diffraction patterns, theoretical calculation results, fluorescence lifetimes, and Movie S1 (molecular domino transformation of **1O**). CCDC 2279131 and 2279132. For ESI and crystallographic data in CIF or other electronic format see DOI: https://doi.org/10.1039/d4tc00406j

mechanism of the transformation are investigated using nanoindentation[24–27] and microcrystal electron diffraction (MicroED) techniques,[28–35] respectively.

Results and discussion

Crystals of **1** were synthesized by a condensation reaction of 4-nitroaniline and salicylaldehyde in ethanol. Recrystallization of **1** from THF resulted in columnar orange crystals (Fig. 1b). Two types of crystals were observed. Upon UV (365 nm) light irradiation, one type emits strong yellow color while the other emits weak orange color. Hereafter, these two crystal polymorphs are referred as **1Y** and **1O**, respectively (Fig. 1c(i)). Such remarkable emission color differences between polymorphs are often observed in molecular crystals showing excited-state intramolecular proton transfer (ESIPT): an intramolecular proton transfer from an excited enol to an excited keto form causes an emission spectral redshift.[16,23,36–38] Their emission spectra were recorded by a fluorescent microscope (IX71, Olympus Co., Ltd.) with a spectrometer (USB4000, Ocean Optics Co., Ltd.) as shown in Fig. 1c(ii). **1Y** exhibits two emission peaks at 567 and 606 nm while **1O** at 614 nm with a shoulder at 580 nm. A shorter fluorescence lifetime of **1O** than that of **1Y** indicates that non-radiative relaxation pathways have a larger contribution to the fluorescence of **1O** than **1Y** (Fig. S4, ESI†). In addition, spatially resolved fluorescent measurements by a hyperspectral camera (SI-108, EBA JAPAN Co., Ltd.), which can get emission spectra at a specific area of a single crystal, revealed their non-uniform emission properties (Fig. 1d). The experimental setup is the same as in the previous report.[39] The relative intensity of the emission peaks around 570 and 610 nm changes depending on measurement points in each single crystal. Note that emission from the edge of **1Y** (region 3 in Fig. d(i)) shows a spectrum resembling that of **1O** when compared to the middle region (region 2 in Fig. d(i)). We surmise that the emission heterogeneity is due to the formation of a mixed crystal of **1Y** with a small portion of **1O**. The ratio of **1O** at the edge is larger than that at the middle. Such kind of intergrowth polymorphs have been investigated by Desiraju and coworkers on aspirin[40] and felodipin[25] molecular crystals.

Interestingly, **1O** shows an emission color change upon mechanical stimuli (Fig. 1e and Movie S1, ESI†). Orange emission from **1O** transformed into yellow at the stimulated area. The yellow emission area gradually spreads over the whole crystal, suggesting the operation of MDT in the crystal[11] that transforms it from **1O** to **1Y**. Propagation of MDT from the stimulated area to an area within a radius of *ca.* 30 μm occurred within one minute. In the next 20 seconds, MDT rapidly proceeded over 200 μm along the long axis of the **1O**. The transformation was also confirmed by spatially resolved emission spectra recorded by a hyperspectral camera and fluorescence lifetime measurements (Fig. S5, ESI†). The emission spectrum obtained at the regions 3 of **1O** in Fig. 1e has strong and relatively weak peaks at 610 and 580 nm, respectively. The relative intensities of the peaks become the opposite after the transformation and the resulting spectrum nearly-corresponds to that of the as-prepared **1Y**. Moreover, increase of the emission intensity by 9.4 times as well as elongation of the fluorescence lifetime after the transformation were confirmed.

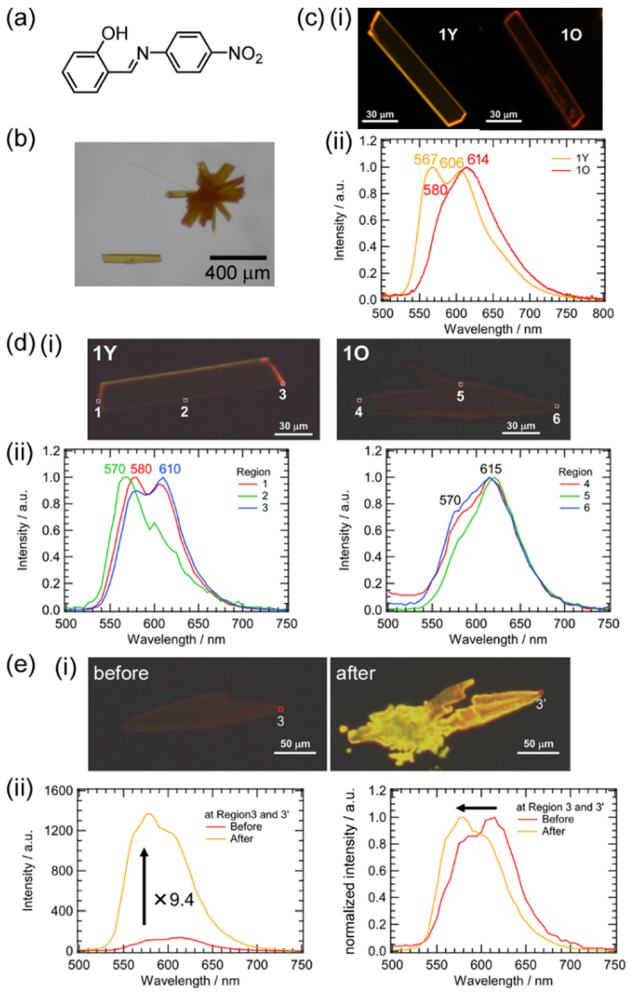

Fig. 1 (a) Molecular structure of **1**. (b) Photographic images of **1** under white light. (c)–(e) (i) Photographic images of **1Y**, **1O**, and **1O** before transformation (before), and after transformation (after) under UV light and (ii) their emission spectra. Emission spectra in (c) were recorded by a fluorescent microscope (IX71, Olympus Co., Ltd.) with a spectrometer (USB4000, Ocean Optics Co., Ltd.) while those in (d) and (e) were measured by a hyperspectral camera (SI-108, EBA JAPAN Co., Ltd.).

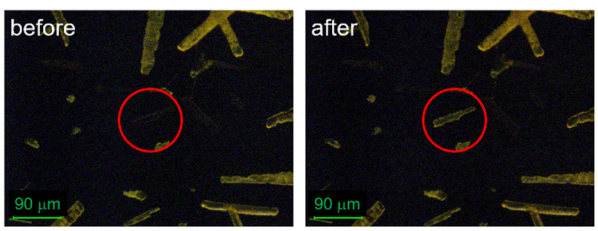

Fig. 2 Photographic images of **1** under UV light before and after nanoindentation (Hysitron TI980, Bruker Corp.). Mechanically stimulated **1O** is circled in red.

Sensitivity of **1O** against mechanical stimuli was investigated using nanoindentation (Fig. 2 and Fig. S8, ESI†).[24–27] **1O** for nanoindentation studies was prepared by evaporation of the THF solution dropped on a glass plate under air at room temperature. More than 20 crystals of **1O** prepared on glass plates were stimulated by a diamond indenter tip with the maximum applied load ranging from 1 to 3000 μN. The transformation of the stimulated crystals was confirmed by emission color change. The large variation in the force required for triggering the transformation could have origins in a variety of factors such as the crystal size, shape, local surface topology, how firmly the crystal is attached to the substrate, and so on. Some crystals showed high mechanical sensitivities, *i.e.*, they underwent the transformation at forces as low as 1 μN.

The origins of the different emission properties and structural stabilities of **1O** and **1Y** were investigated based on their crystal structures.[41,42] Due to **1O**'s mechanical sensitivity to transform into **1Y**, large single crystals of **1O** could not be mounted on a conventional X-ray diffractometer. Thus, the crystal structures of **1O** and **1Y** were determined by microcrystal electron diffraction (MicroED) (Fig. 3 and 4).[28–35] For this purpose, microcrystalline **1O** and **1Y** were prepared directly on a copper EM grid (Quantifoil R1.2/1.3 Cu 200 mech) by 'painting' the THF solution, not crystal suspension, using a brush to prevent any possible mechanical stimulation of the crystals and loaded onto a Talos Arctica microscope (Thermo Fisher Scientific) equipped with a Ceta detector (CMOS 4k × 4k, Thermo Fisher Scientific). Data collection was performed using SerialEM[43] with a strategy described in the literature.[34,35,44,45] Diffraction patterns from more than 1150 crystals were measured at 200 kV with an electron flux of 0.05 e^{-} $Å^{-2}$ s^{-1}. Diffraction patterns were indexed, integrated, and scaled using DIALS.[46–48] First, crystals were indexed without using any prior cell information and the Bravais lattice constraints. The distribution of the resulting unit cell parameters indicated the presence of two crystal forms (monoclinic and orthorhombic) in the sample (ESI,† Fig. S2). Next, the dataset was reprocessed twice, using the cell parameter and lattice type of each crystal form. Crystals in each group were further clustered by xia2.multiplex[49] to find the best sets of crystals for final merging (Tables S1 and S2, ESI†). 697 crystals were indexed in the monoclinic crystal form and 55 good crystals were merged. The structure was solved in the space group $P2_1/c$ and was identical to the **1Y** structure solved using X-ray diffraction (XRD) in previous studies.[50,51] The powder XRD pattern of **1Y** agrees well with that simulated from the solved structure (Fig. S3, ESI†). The other 90 crystals were indexed in the new orthorhombic crystal form and the 4 best crystals gave a structure in the $Pna2_1$ space group. We assigned this to be **1O**. The crystal structures were solved using SHELXT[52] and refined kinematically by SHELXL[53] in Olex2 GUI (Table S3, ESI†).[54,55]

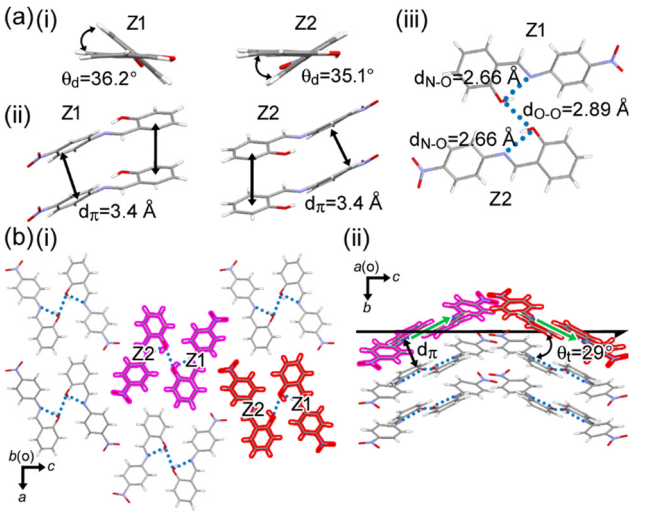

Fig. 3 (a) (i) Dihedral angle, θ_d, between the two phenyl rings, (ii) distances between π-stacked molecules, (iii) hydrogen-bonding dimer, (b) (i) packing diagram, and (ii) side view of a right-handed two-fold helix by neighboring columns in **1O**. The helical handedness is defined by tilt (green arrow) of the dimer according to the supramolecular-tilt-chirality method.[60–62]

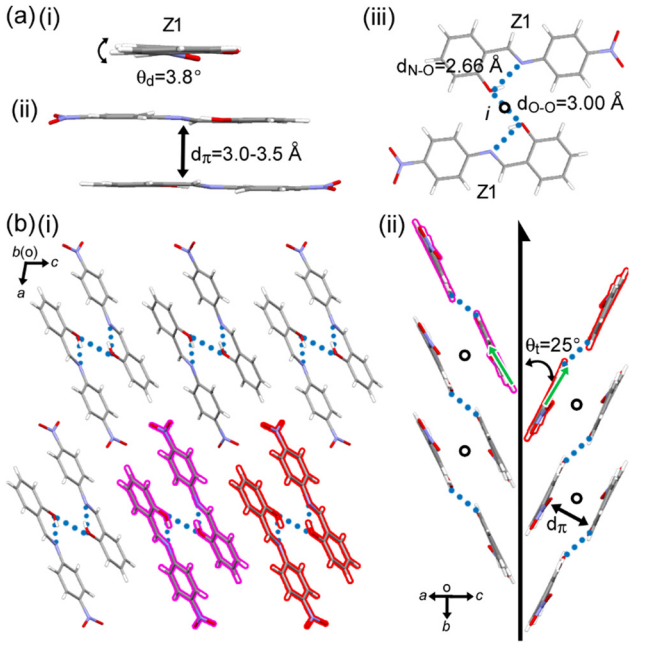

Fig. 4 (a) (i) Dihedral angle between the two phenyl rings, (ii) distance between π-stacked molecules, (iii) hydrogen-bonding dimer, (b) (i) packing diagram, and (ii) side view of a right-handed two-fold helix by neighbouring columns in **1Y**. The helical handedness is defined by tilt (green arrow) of the dimer according to the supramolecular-tilt-chirality method.[60–62]

There are two crystallographically independent molecules of Z1 and Z2 in **1O**; the dihedral angles between the two phenyl groups in them are θ_d = 36.2° and 35.1°, respectively (Fig. 3a(i)). Such large θ_d could be one of the origins of the low emission intensity due to twisted intramolecular charge transfer.[23,37,56–59] The π–π distance (d_π) between Z1 (or Z2) molecules is *ca.* 3.4 Å (Fig. 3a(ii)). In addition to the intramolecular hydrogen-bonding between hydroxyl and imino groups (N···O distance of d_{N-O} = 2.66 Å), **1** forms an intermolecular hydrogen bond between the hydroxyl groups (O···O distance of d_{O-O} = 2.89 Å) of Z1 and Z2 to afford a hydrogen-bonded dimer (Fig. 3a(iii)). The dimer tilts *ca.* 29° against the *c* axis and stacks along the *b* axis with a distance of d_π = 3.4 Å to form a columnar assembly (Fig. 3b). Two-fold helices in **1O** are perpendicular to the stacking direction.

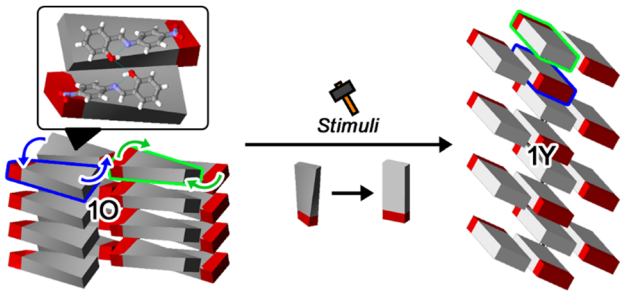

Fig. 5 Schematic representation of the MDT mechanism from **1O** to **1Y**.

In contrast to **1** in **1O**, **1** in **1Y** is almost planar, *i.e.*, the two phenyl groups are nearly parallel (θ_d = 3.8°) (Fig. 4a(i)). This value is much smaller than that noted in **1O** (θ_d = 36.2°, 35.1°). Consistent with a previous report by Borbone *et al.*[23] θ_d and fluorescence lifetime are correlated, *i.e.*, smaller dihedral angles result in longer fluorescence lifetime. d_π between Z1 molecules is 3.0–3.5 Å (Fig. 4a(ii)). Similar to **1O**, **1** forms a hydrogen-bonding dimer with intra- and inter-molecular hydrogen-bonding N···O (d_{N-O} = 2.66 Å) and O···O (d_{O-O} = 3.00 Å), respectively (Fig. 4a(iii)). The dimer tilts *ca.* θ_t = 25° against the *b* axis and stacks with an inversion symmetry at d_π = 3.0–3.5 Å along the *b* axis to form a columnar assembly. Neighbouring columns are related by a two-fold helical symmetry along the stacking direction in a herringbone manner (Fig. 4b). The π-stacking manner of **1** is parallel in **1O** while that in **1Y** is antiparallel.

Based on the crystallographic studies, the domino transformation from **1O** to **1Y** coupled with an emission change is described by molecular conformational changes as well as molecular rearrangement in the crystal lattice. Phenyl rings rotate more than 30° during MDT, *i.e.*, from θ_d = 36.2° and 35.1° in **1O** to θ_d = 3.8° in **1Y**. One of the possible molecular movements is schematically shown in Fig. 5. Hydrogen-bonding dimers in a column rotate clockwise or counterclockwise along with the conformational change. As a result, the dimers in a column and those in the neighbouring column stack alternately to form **1Y**. Interestingly, electron microscope images of **1Y** crystals often had cracks in the middle and/or jagged ends, while **1O** crystals tended to be straighter (Fig. S1, ESI†). This might have resulted from internal stress caused by the transformation.

The domino transformation from **1O** to **1Y** by mechanical stimuli suggests that **1Y** is more stable than **1O**. The relative stability was evaluated by DFT calculations using the Quantum ESPRESSO program (Fig. S7 and Tables S4, S5, ESI†).[63–65] The calculated lattice energies ($E_{lattice}$) of **1O** (n = 8) and **1Y** (n = 4) are 228.3 and 116.4 kcal mol^{-1}, respectively. The $E_{lattice}$ values per molecule ($E_{lattice}/n$) for **1O** and **1Y** are 28.5 and 29.1 kcal mol^{-1}, respectively, which shows that **1Y** is more stable than **1O**. Heating under an optical microscope showed that **1O** melts at lower temperature (*ca.* 120 °C) than **1Y** (*ca.* 160 °C), also suggesting the stability order.

Effects of the conformation (**1** is planar in **1Y**, while twisted in **1O**) on fluorescence spectra were studied by time dependent DFT calculations using the Gaussian program.[66] The torsional angles of four rotatable bonds were fixed in the geometry optimizations in the excited state. The optimized structures show that **1** has a *keto* form in the excited state (Fig. S7, ESI†). Although the calculated wavelengths of the fluorescence spectra are 50–70 nm longer than the experimental ones, the calculated wavelength in **1O** is longer than that in **1Y**, which agrees with experiments (Table S6, ESI†). This result indicates a crucial role of molecular conformation (twisting of two benzene rings) on the emission spectral redshift in **1O**.

Conclusions

In conclusion, we discovered and characterized a Schiff base crystal of **1** showing mechanically-induced molecular domino transformation (MDT). Spectrometry revealed changes in emission color and intensity by the transformation (peak top shift of *ca.* 50 nm and over 9-fold increase of the intensity). Nanoindentation studies quantified the absolute values of the mechanical force necessary for the transformation (1 μN at the smallest). **1** is attractive as a sensing material because of the mechanical sensitivity and large emission change. MDT amplifies a local stimulus to a response by the whole crystal. Atomic level insights of the transformation mechanism were obtained by solving the crystal structure of a metastable **1O** by MicroED. Other series of Schiff bases, which show polymorph-dependent emission differences, are under investigation to rationally improve and control properties suitable for sensing applications based on the fundamental understanding of MDT.

Author contributions

TS, TN, AK, TN and GK contributed in sample preparation and crystallographic studies. YF and FI contributed in fluorescent measurements. YZ and UR contributed in nanoindentation measurements. ST contributed in DFT calculations. NK contributed in ^{1}H NMR, ^{13}C NMR and HR-MS. TS and RT initiated the project. TS wrote the draft and all of the authors contributed in finalizing the manuscript.

Conflicts of interest

There are no conflicts to declare.

Acknowledgements

This work was supported by JSPS KAKENHI Grant Number 22K05054 for T. S. and Research Support Project for Life Science and Drug Discovery (BINDS) from AMED under Grant Number JP22ama121001. R. T. thanks the Science and Engineering Research Board for funding under the Teachers Associateship for Research Excellence (TARE) grant (Project No. TAR/2021/000251). We thank Dr Yanagisawa and Dr Yamashita for their advice on semi-automatic MicroED data collection with SerialEM macros. We are also grateful to Dr Suzuki for pre-evaluation of crystals for MicroED by a fluorescence microscope.

Notes and references

1 P. Bamfield and M. G. Hutching, *Chromic Phenomena: Technological Applications of Colour Chemistry*, Royal Society of Chemistry, 2nd edn, 2010.
2 M. Kato, H. Ito, M. Hasegawa and K. Ishii, *Chem. – Eur. J.*, 2019, **25**, 5105.
3 Y. Zheng, X. Jia, K. Li, J. Xu and X.-H. Bu, *Adv. Energy Mater.*, 2021, 2100324.
4 M. D. Cohen, G. M. J. Schmidt and S. Flavian, *J. Chem. Soc.*, 1964, 2041.
5 J. Bregman, L. Leiserowitz and G. M. J. Schmidt, *J. Chem. Soc.*, 1964, 2068.
6 T. Mutai, H. Satou and K. Araki, *Nat. Mater.*, 2005, **4**, 685.
7 T. Mutai, H. Tomoda, T. Ohkawa, Y. Yabe and K. Araki, *Angew. Chem., Int. Ed.*, 2008, **47**, 9522.
8 Y. Hino and S. Hayashi, *Chem. – Eur. J.*, 2021, **27**, 17595.
9 M. Fukushima, K. Sato, Y. Fujimoto, F. Ito and R. Katoh, *Cryst. Growth Des.*, 2022, **22**, 2071.
10 Y. Sagara, T. Mutai, I. Yoshikawa and K. Araki, *J. Am. Chem. Soc.*, 2007, **129**, 1520.
11 H. Ito, M. Muromoto, S. Kurenuma, S. Ishizaka, N. Kitamura, H. Sato and T. Seki, *Nat. Commun.*, 2013, **4**, 2009.
12 M. Jin, T. Sumitani, H. Sato, T. Seki and H. Ito, *J. Am. Chem. Soc.*, 2018, **140**, 2875.
13 S. Hayashi and T. Koizumi, *Angew. Chem., Int. Ed.*, 2016, **55**, 2701.
14 T. Mutai, T. Sasaki, S. Sakamoto, I. Yoshikawa, H. Houjou and S. Takamizawa, *Nat. Commun.*, 2020, **11**, 1824.
15 B. Bhattacharya, D. Roy, S. Dey, A. Puthuvakkal, S. Bhunia, S. Mondal, R. Chowdhury, M. Bhattacharya, M. Mandal, K. Manoj, P. K. Mandal and C. M. Reddy, *Angew. Chem., Int. Ed.*, 2020, **59**, 19878.
16 E. Hadjoudis and I. M. Mavridis, *Chem. Soc. Rev.*, 2004, **33**, 579.
17 K. Amimoto and T. Kawato, *J. Photochem. Photobiol., C*, 2005, **6**, 207.
18 S. Kobatake, S. Takami, H. Muto, T. Ishikawa and M. Irie, *Nature*, 2007, **446**, 778.
19 M. Kato, A. Omura, A. Toshikawa, S. Kishi and Y. Sugimoto, *Angew. Chem., Int. Ed.*, 2002, **41**, 3183.
20 T. Ogoshi, Y. Shimada, Y. Sakata, S. Akine and T. A. Yamagishi, *J. Am. Chem. Soc.*, 2017, **139**, 5664.
21 I. Hisaki, Y. Suzuki, E. Gomez, Q. Ji, N. Tohnai, T. Nakamura and A. Douhal, *J. Am. Chem. Soc.*, 2019, **141**, 2111.
22 Z. Zhang, X. Song, S. Wang, F. Li, H. Zhang, K. Ye and Y. Wang, *J. Phys. Chem. Lett.*, 2016, **7**, 1697.
23 F. Borbone, A. Tuzi, B. Panunzi, S. Piotto, S. Concilio, R. Shikler, S. Nabha and R. Centore, *Cryst. Growth Des.*, 2017, **17**, 5517.
24 S. Varughese, M. S. R. N. Kiran, U. Ramamurty and G. R. Desiraju, *Angew. Chem., Int. Ed.*, 2013, **52**, 2701.
25 M. K. Mishra, G. R. Desiraju, U. Ramamurty and A. D. Bond, *Angew. Chem., Int. Ed.*, 2014, **53**, 13102.
26 M. K. Mishra, U. Ramamurty and G. R. Desiraju, *Curr. Opin. Solid State Mater. Sci.*, 2016, **20**, 361.
27 R. Devarapalli, S. B. Kadambi, C.-T. Chen, G. R. Krishna, B. R. Kammari, M. J. Buehler, U. Ramamurty and C. M. Reddy, *Chem. Mater.*, 2019, **31**, 1391.
28 T. Gruene, J. T. C. Wennmacher, C. Zaubitzer, J. J. Holstein, J. Heidler, A. Fecteau-Lefebvre, S. De Carlo, E. Müller, K. N. Goldie, I. Regeni, T. Li, G. Santiso-Quinones, G. Steinfeld, S. Handschin, E. van Genderen, J. A. van Bokhoven, G. H. Clever and R. Pantelic, *Angew. Chem., Int. Ed.*, 2018, **57**, 16313.
29 S. Ito, F. J. White, E. Okunishi, Y. Aoyama, A. Yamano, H. Sato, J. D. Ferrara, M. Jasnowski and M. Meyer, *CrystEngComm*, 2021, **23**, 8622.
30 C. G. Jones, M. W. Martynowycz, J. Hattne, T. J. Fulton, B. M. Stoltz, J. A. Rodriguez, H. M. Nelson and T. Gonen, *ACS Cent. Sci.*, 2018, **4**, 1587.
31 J. A. Newman, L. Iuzzolino, M. Tan, P. Orth, J. Bruhn and A. Y. Lee, *Mol. Pharm.*, 2022, **19**, 2133.
32 M. Lightowler, S. Li, X. Ou, X. Zou, M. Lu and H. Xu, *Angew. Chem., Int. Ed.*, 2022, **61**, e202114985.
33 J. Hitchen, I. Andrusenko, C. L. Hall, E. Mugnaioli, J. Potticary, M. Gemmi and S. R. Hall, *Cryst. Growth Des.*, 2022, **22**, 1155.
34 T. Sasaki, T. Nakane, A. Kawamoto, T. Nishizawa and G. Kurisu, *CrystEngComm*, 2023, **25**, 352.
35 D. Gogoi, T. Sasaki, T. Nakane, A. Kawamoto, H. Hojo, G. Kurisu and R. Thakuria, *Cryst. Growth Des.*, 2023, **23**, 5821.
36 T. Mutai, H. Shono, Y. Shigemitsu and K. Araki, *CrystEngComm*, 2014, **16**, 3890.
37 H. Konoshima, S. Nagao, I. Kiyota, K. Amimoto, N. Yamamoto, M. Sekine, M. Nakata, K. Furukawa and H. Sekiya, *Phys. Chem. Chem. Phys.*, 2012, **14**, 16778.
38 V. S. Padalkar and S. Seki, *Chem. Soc. Rev.*, 2016, **45**, 169.
39 S. Katsumi, M. Saigusa and F. Ito, *J. Phys. Chem. B*, 2022, **126**, 976.
40 A. D. Bond, R. Boese and G. R. Desiraju, *Angew. Chem., Int. Ed.*, 2007, **46**, 618.
41 Deposition numbers CCDC 2279131/COD-3000450 (for **1O**) and CCDC 2279132/COD-3000451 (for **1Y**) contain the supplementary crystallographic data for this paper†.
42 Raw diffraction images of 1O and 1Y XRDa-142 are provided free of charge by Xtal Raw Data Archive (XRDa). Scripts for MicroED data collection and processing are available at **https://github.com/GKLabIPR/MicroED**.
43 C. J. H. Smalley, H. E. Hoskyns, C. E. Hughes, D. N. Johnstone, T. Willhammar, M. T. Young, C. J. Pickard, A. J. Logsdail, P. A. Midgley and K. D. M. Harris, *Chem. Sci.*, 2022, **13**, 5277.
44 H. Lu, T. Nakamuro, K. Yamashita, H. Yanagisawa, O. Nureki, M. Kikkawa, H. Gao, J. Tian, R. Shang and E. Nakamura, *J. Am. Chem. Soc.*, 2020, **142**, 18990.
45 H. Hamada, T. Nakamuro, K. Yamashita, H. Yanagisawa, O. Nureki, M. Kikkawa, K. Harano, R. Shang and E. Nakamura, *Bull. Chem. Soc. Jpn.*, 2020, **93**, 776.
46 G. Winter, D. G. Waterman, J. M. Parkhurst, A. S. Brewster, R. J. Gildea, M. Gerstel, L. Fuentes-Montero, M. Vollmar, T. Michels-Clark, I. D. Young, N. K. Sauter and G. Evans, *Acta Crystallogr., Sect. D: Struct. Biol.*, 2018, **74**, 85.
47 M. T. B. Clabbers, T. Gruene, J. M. Parkhurst, J. P. Abrahams and D. G. Waterman, *Acta Crystallogr., Sect. D: Struct. Biol.*, 2018, **74**, 506.
48 J. Beilsten-Edmands, G. Winter, R. Gildea, J. Parkhurst, D. Waterman and G. Evans, *Acta Crystallogr., Sect. D: Struct. Biol.*, 2020, **76**, 385.

49 R. J. Gildea, J. Beilsten-Edmands, D. Axford, S. Horrell, P. Aller, J. Sandy, J. Sanchez-Weatherby, C. D. Owen, P. Lukacik, C. Strain-Damerell, R. L. Owen, M. A. Walsh and G. Winter, *Acta Crystallogr., Sect. D: Struct. Biol.*, 2022, **78**, 752.
50 J. Burgess, J. Fawcett, D. R. Russell, S. R. Gilani and V. Palma, *Acta Crystallogr., Sect. C: Cryst. Struct. Commun.*, 1999, **55**, 1707.
51 T. Kondori, N. Akbarzadeh-T, M. Fazli, B. Mir, M. Dušek and V. Eigner, *J. Mol. Struct.*, 2021, **1226**, 129395.
52 G. M. Sheldrick, *Acta Crystallogr., Sect. A: Found. Adv.*, 2015, **71**, 3.
53 G. M. Sheldrick, *Acta Crystallogr., Sect. C: Struct. Chem.*, 2015, **71**, 3.
54 O. V. Dolomanov, L. J. Bourhis, R. J. Gildea, J. A. K. Howard and H. Puschmann, *J. Appl. Cryst.*, 2009, **42**, 339.
55 L. J. Bourhis, O. V. Dolomanov, R. J. Gildea, J. A. K. Howard and H. Puschmann, *Acta Crystallogr., Sect. A: Found. Crystallogr.*, 2015, **71**, 59.
56 M. I. Knyazhansky, A. V. Metelitsa, A. J. Bushkov and S. M. Aldoshin, *J. Photochem. Photobiol., A*, 1996, **97**, 121.
57 Z. R. Grabowski, K. Rotkiewicz and W. Rettig, *Chem. Rev.*, 2003, **103**, 3899.
58 S. Sasaki, G. P. C. Drummen and G.-I. Konishi, *J. Mater. Chem. C*, 2016, **4**, 2731.
59 J. Shi, S.-J. Yoon, L. Viani, S. Y. Park, B. Milián-Medina and J. Gierschner, *Adv. Opt. Mater.*, 2017, **5**, 1700340.
60 I. Hisaki, T. Sasaki, N. Tohnai and M. Miyata, *Chem. – Eur. J.*, 2012, **18**, 10066.
61 T. Sasaki, I. Hisaki, T. Miyano, N. Tohnai, K. Morimoto, H. Sato, S. Tsuzuki and M. Miyata, *Nat. Commun.*, 2013, **4**, 1787.
62 M. Miyata, N. Tohnai, I. Hisaki and T. Sasaki, *Symmetry*, 2015, **7**, 1914.
63 P. Giannozzi, S. Baroni, N. Bonini, M. Calandra, R. Car, C. Cavazzoni, D. Ceresoli, G. L. Chiarotti, M. Cococcioni, I. Dabo, A. Dal Corso, S. de Gironcoli, S. Fabris, G. Fratesi, R. Gebauer, U. Gerstmann, C. Gougoussis, A. Kokalj, M. Lazzeri, L. Martin-Samos, N. Marzari, F. Mauri, R. Mazzarello, S. Paolini, A. Pasquarello, L. Paulatto, C. Sbraccia, S. Scandolo, G. Sclauzero, A. P. Seitsonen, A. Smogunov, P. Umari and R. M. Wentzcovitch, *J. Phys.: Condens. Matter*, 2009, **21**, 395502.
64 P. Giannozzi, O. Andreussi, T. Brumme, O. Bunau, M. Buongiorno Nardelli, M. Calandra, R. Car, C. Cavazzoni, D. Ceresoli, M. Cococcioni, N. Colonna, I. Carnimeo, A. Dal Corso, S. de Gironcoli, P. Delugas, R. A. DiStasio, A. Ferretti, A. Floris, G. Fratesi, G. Fugallo, R. Gebauer, U. Gerstmann, F. Giustino, T. Gorni, J. Jia, M. Kawamura, H.-Y. Ko, A. Kokalj, E. Küçükbenli, M. Lazzeri, M. Marsili, N. Marzari, F. Mauri, N. L. Nguyen, H.-V. Nguyen, A. Otero-de-la-Roza, L. Paulatto, S. Poncé, D. Rocca, R. Sabatini, B. Santra, M. Schlipf, A. P. Seitsonen, A. Smogunov, I. Timrov, T. Thonhauser, P. Umari, N. Vast, X. Wu and S. Baroni, *J. Phys.: Condens. Matter*, 2017, **29**, 465901.
65 T. Sasaki, T. Nakane, A. Kawamoto, Y. Zhao, Y. Fujimoto, T. Nishizawa, S. Tsuzuki, F. Ito, U. Ramamurty, R. Thakuria and G. Kurisu, Data for ''Mechanically-Sensitive Fluorochromism by Molecular Domino Transformation in a Schiff Base Crystal'', *zenodo*, 2024, DOI: **10.5281/zenodo.10476969**.
66 M. J. Frisch, G. W. Trucks, H. B. Schlegel, G. E. Scuseria, M. A. Robb, J. R. Cheeseman, G. Scalmani, V. Barone, G. A. Petersson, H. Nakatsuji, X. Li, M. Caricato, A. V. Marenich, J. Bloino, B. G. Janesko, R. Gomperts, B. Mennucci, H. P. Hratchian, J. V. Ortiz, A. F. Izmaylov, J. L. Sonnenberg, D. Williams-Young, F. Ding, F. Lipparini, F. Egidi, J. Goings, B. Peng, A. Petrone, T. Henderson, D. Ranasinghe, V. G. Zakrzewski, J. Gao, N. Rega, G. Zheng, W. Liang, M. Hada, M. Ehara, K. Toyota, R. Fukuda, J. Hasegawa, M. Ishida, T. Nakajima, Y. Honda, O. Kitao, H. Nakai, T. Vreven, K. Throssell, J. A. Montgomery Jr, J. E. Peralta, F. Ogliaro, M. J. Bearpark, J. J. Heyd, E. N. Brothers, K. N. Kudin, V. N. Staroverov, T. A. Keith, R. Kobayashi, J. Normand, K. Raghavachari, A. P. Rendell, J. C. Burant, S. S. Iyengar, J. Tomasi, M. Cossi, J. M. Millam, M. Klene, C. Adamo, R. Cammi, J. W. Ochterski, R. L. Martin, K. Morokuma, O. Farkas, J. B. Foresman and D. J. Fox, *Gaussian 16, Revision A.03*, Gaussian Inc., Wallingford CT, 2016.